TTI DIT for dirty salt inversion in the Mississippi Canyon area, Gulf of Mexico

John DeLaughter and Michael Harbin, Murphy Oil Corp.; Dawn Herrington, Ecopetrol America Inc.; Andrey A. Ortega, Seung Yoo, Taejong Kim, Will Whiteside and Cristina Reta-Tang, TGS*

Summary

For deep-water Gulf of Mexico, accurate salt geometry is critical for subsalt imaging. This requires the definition of both external and internal salt geometries. In recent years, external salt geometry has been improved due to advances in wide azimuth acquisition, long-offset recording, velocity model building, and migration algorithms. In this paper we present the results of dirty salt inversion using TTI RTM technology based on DIT scans.

Approximately 42 OCS blocks of the Freedom survey located in the Mississippi Canyon area of the Gulf of Mexico were imaged. The study area was previously imaged with VTI Kirchhoff and RTM technology using a constant salt velocity. Application of TTI DIT for dirty salt using a laterally heterogenous salt velocity has resulted in better base of salt definition and improved subsalt images. Results indicate that intra-salt velocity is slower than salt velocity.

Introduction

Different types of dirty salt schemes have been attempted to invert for intra-salt inclusions in order to improve the image quality in the subsalt regime. Among those, full wave form inversion (Tarantola 1984, Zhang and Wang, 2009), RTM based delayed-imaging-time scan (Wang et al., 2009), reflectivity methods (Ji et al., 2010), and ray-based tomography methods using RTM 3D angle gathers (Li et al., 2011). Dirty salt multi-azimuth tomography methods based on residual moveout may yield good results if there are enough reflections within the salt. However, if the reflection angle is not wide enough or if inclusions are too small and spatially sparse it may lead the global inversion tomography approach to incorrect velocity updates. Thus reflection-based methods may require a large number of iterations before converging on a result.

On the other hand, the RTM based DIT scan method is computationally attractive since it requires only a single RTM pass and it is based on focusing analysis. The zero time imaging condition generates the conventional RTM image, while the positive and negative nonzero-time imaging condition generates a scan of images called DIT scans. For this paper we generated 21 DIT images and applied the RTM based delayed-time scan method to derive intra-salt velocities in wide azimuth data from the Gulf of Mexico.

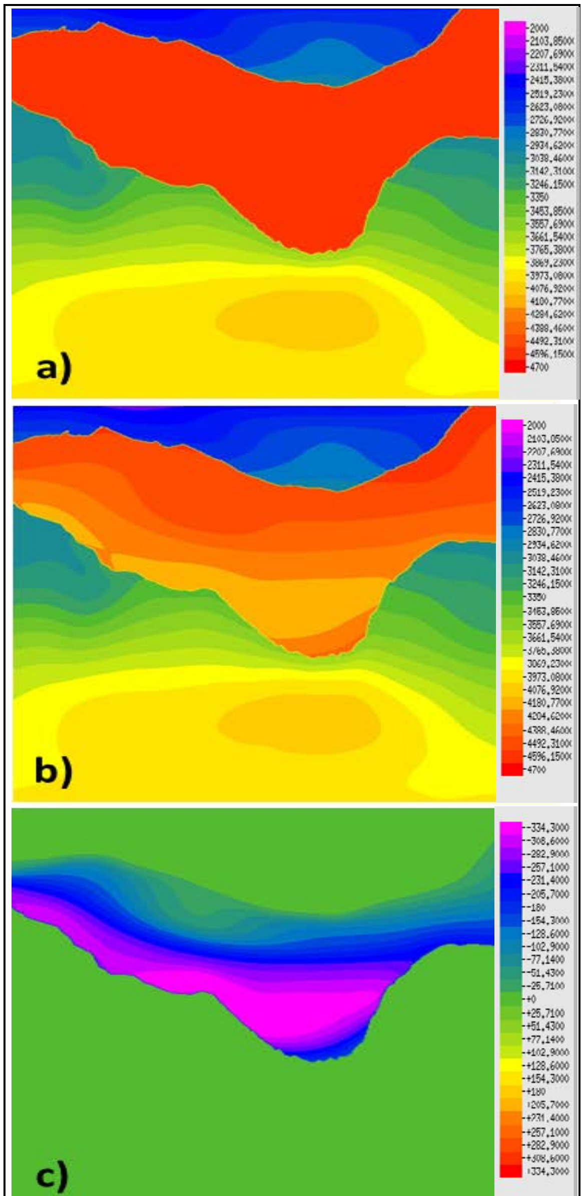

Figure 1: a) Initial velocity model, b) Updated velocity model derived by TTI DIT method and c) Velocity perturbation.

DOI http://dx.doi.org/10.1190/segam2014-1553.1

Method

We applied DIT for dirty salt velocity inversion to a 3D field data in Mississippi Canyon. Figures 1a and 1b show the subsalt velocity model before and after the RTM-based subsalt DIT scan. A total of 21 RTM-based DIT scan images were produced. The initial velocity model was derived in the upper basins after three iterations of high resolution tomography to update the supra-salt sediment velocity model. For each tomography iteration, 3D TTI pre-stack Kirchhoff depth migration was used to generate image gathers. Automatic residual curvature analysis on the resulting image gathers and dip estimation on the PSDM stack were computed for use in tomography. Rays passing through salt were masked out during raytracing. Using a multi-scale iterative approach, the velocity along the symmetry axis V_o was updated. Long wavelength velocity variations were inverted first. Short wavelength velocity features were gradually added in subsequent tomography iterations. Gather flatness, event focusing, and well ties were evaluated after each tomography iteration. The supra-salt velocity model was validated against check-shot velocities and salt top picks. The salt top picks from wells match with the PSDM seismic within less than 1% error. Therefore, no further tomography updates were needed on the anisotropy values of ε and δ.

Using an automatic subsalt DIT picking tool, DITs were picked by comparing scan panels (stacked images) and gather displays. Velocities inside the salt body decreased by as much as 334 m/s after the subsalt velocity update (see Figure 1c). Figures 2a and 2b shows the corresponding initial RTM stack and the RTM image obtained by the initial and the updated velocity model that produces the best focused image from DIT panels. Most changes occurred in places with relatively large velocity updates. There are significant improvements to image quality for layering and inclusions in the salt and better base salt definition as well as substantial re-depthing and better imaging of subsalt events.

Figures 3a and 3b shows a comparison of the previous multi-client VTI velocity model with constant salt velocity and our final velocity model with dirty salt including subsalt velocity updates. The subsalt velocity field is more nuanced and shows clear geological influence after use of dirty salt. Finally, Figures 3c and 3d show the corresponding RTM migrated images using the velocity models in Figures 3a and 3b, respectively. Both base salt definition and focusing of subsalt features have been enhanced by use of a dirty salt model. A further increase in vertical resolution in Figure 3d is due to the application of broadband Clari-Fi technology.

Conclusions

The application of TTI DIT for dirty salt in the Mississippi Canyon area has produced significant improvement in the focusing and lateral continuity of images including better definition of the intra-salt layering and inclusions, and enhanced base salt geometry as well as more continuous and stronger subsalt events. As expected, results indicate that dirty salt velocity is smaller than salt velocity.

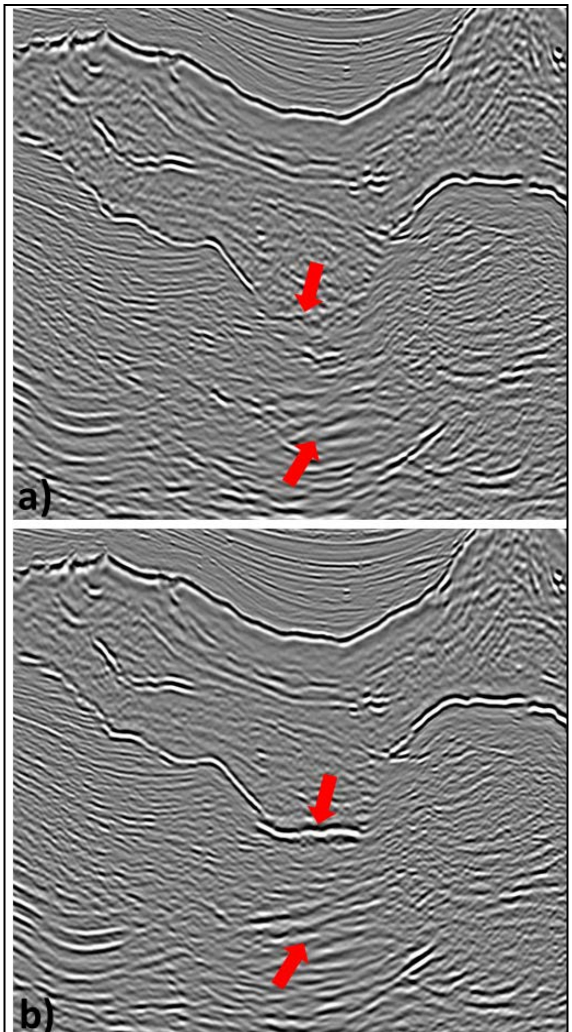

Figure 2: a) Initial RTM stack and b) RTM stack using updated TTI DIT scan velocity model. Notice the improvement in the base of salt as well as the much better lateral continuity of the reflector in the subsalt regime. The focusing of intrasalt reflectivity has also been improved. Maximum RTM frequency is 20 Hz.

DOI http://dx.doi.org/10.1190/segam2014-1553.1

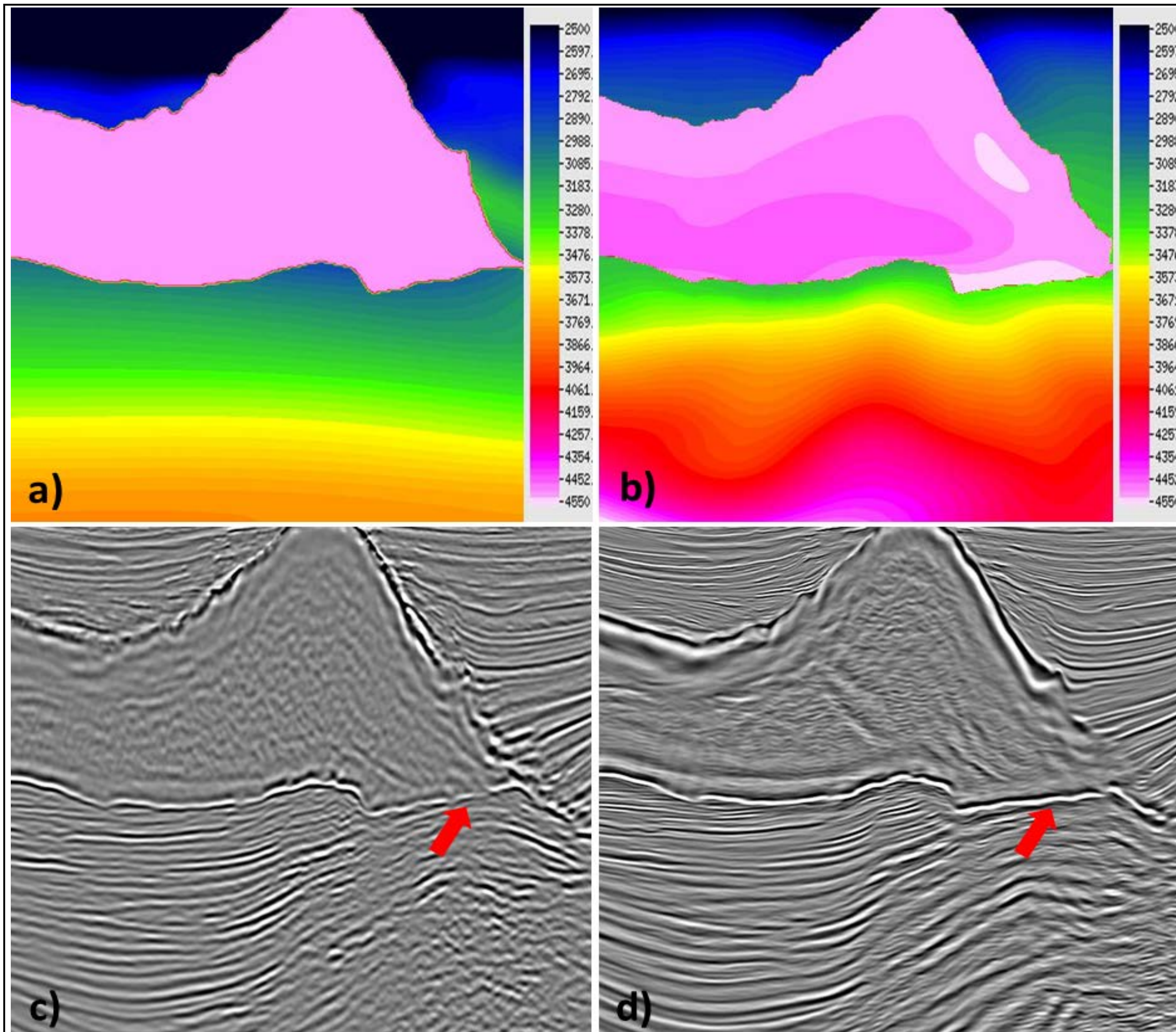

Figure 3: a) Previous multi-client VTI velocity model with constant salt velocity, b) TTI velocity model with dirty salt velocity, c) previous multi-client VTI RTM stack (maximum frequency 25 Hz) with constant salt velocity, and d) TTI RTM image (maximum 35 Hz) with dirty salt velocity. Better focusing of the base of salt is clearly demonstrated.

Acknowledgements

The authors would like to thank TGS, Murphy Corporation, and Ecopetrol America Inc. for their permission to publish this work. Thanks to Suresh Nistala and Hao Xun for their contributions in building the initial sedimentary model and to Connie VanSchuyver for reviewing the manuscript.

DOI http://dx.doi.org/10.1190/segam2014-1553.1

http://dx.doi.org/10.1190/segam2014-1553.1

EDITED REFERENCES

Note: This reference list is a copy-edited version of the reference list submitted by the author. Reference lists for the 2014 SEG Technical Program Expanded Abstracts have been copy edited so that references provided with the online metadata for each paper will achieve a high degree of linking to cited sources that appear on the Web.

REFERENCES

Li, Z., S. Ji, B. Bai, Q. Wu, and W. Han, 2011, Dirty salt tomography using RTM 3D angle gathers: 81st Annual International Meeting, SEG, Expanded Abstracts, 4020–4024.

Ji, S., T. Huang, K. Fu, and Z. Li, 2011, Dirty salt velocity inversion: The road to a clearer subsalt image: Geophysics, **76**, no. 5, WB169–WB174.

Tarantola, A., 1984, Inversion of seismic reflection data in the acoustic approximation: Geophysics, **49**, 1259–1266, http://dx.doi.org/10.1190/1.1441754.

Wang, B., C. Mason, M. Guo, K. Yoon, J. Cai, J. Ji, and Z. Li, 2009, Subsalt velocity update and composite imaging using reverse-time-migration based delayed-imaging-time scan: Geophysics, **74**, no. 6, WCA159–WCA166, http://dx.doi.org/10.1190/1.3227152.

Zhang, Y., and D. Wang, 2009, Traveltime information-based wave-equation inversion: Geophysics, **74**, no. 6, WCC27–WCC36, http://dx.doi.org/10.1190/1.3243073.